Organic–Inorganic Hybrids

DOI: 10.1002/ange.200501924

Molecular and Polymeric Hybrids Based on Covalently Linked Polyoxometalates and Transition-Metal Complexes**

Jeonghee Kang, Bubin Xu, Zhonghua Peng, Xiaodong Zhu, Yongge Wei, and Douglas R. Powell*

We report a rational synthetic approach to novel molecular and polymeric hybrids containing polyoxometalate (POM) clusters and transition-metal complexes covalently linked by an organic π-conjugated bridge. There continues to be extensive interest in hybrids containing both POMs and organometallic components.[1–3] The motivation lies not only in chemists' steady desire to bring different structural units together but also in the prospect of generating new functional and multifunctional materials,[4] although the overwhelming interest in organometallic/POM hybrids has so far been focused to their catalytic activity.[1,5] A significant number of organometallic/POM hybrids have already been reported, most of which anchor the organometallic component by either the surface oxygen atoms of POM clusters or active metal centers incorporated within the POM cluster.[1–5] The commonly adopted synthetic approach relies on a self-assembly process in which attachment of the organometallic component and assembly of the POM cluster occur simultaneously.[1–5] Although various other preparation methods have been reported,[6] one which allows rational design and predetermination of structure and properties remains elusive.

One fascinating aspect of POM clusters is their structural diversity, not only in the cluster frame itself but also in the ways of derivatizing them.[1] Among the many types of organically functionalized POMs, organoimido derivatives are particularly interesting.[7] Aside from remarkable stability of the imido metal–nitrogen linkage, which makes further structural modification on the cluster-anchored organic component possible,[8] delocalization of organic π electrons on the POM cluster may lead to a new class of electronic hybrid materials.[9] Indeed, we have recently shown that organoimido derivatives with remote functionality can be used as building blocks to construct hybrid dumbbells,[10] charge-transfer hybrids,[11] and polymer hybrids[12] which have been demonstrated to be photovoltaic materials. Here we report that the building block approach can be extended to the preparation of organometallic POMs with predetermined structures. In particular, we describe the synthesis and optical properties of the first molecular and polymeric hybrids (**3** and **6** in Schemes 1 and 2, respectively) in which POM clusters and transition-metal complexes are linked by an organic π-conjugated bridge. Such hybrids were designed to take advantage of the metal-to-ligand charge-transfer (MLCT) transitions of transition-metal complexes,[13] the electron-accepting properties of POM clusters, and the charge-transport properties of π-conjugated systems, to realize systems with efficient photoinduced charge separation.

Schemes 1 and 2 show the structures and syntheses of molecular hybrid **3** and polymeric hybrid **6**, respectively. Polyoxometalate clusters functionalized with one or two iodo functional groups (**1** and **4**, respectively) were prepared according to previously reported procedures.[14,15] Pd-catalyzed coupling of 4′-ethynyl-2,2′,6′,2″-terpyridine with **1** and **4** yielded terpyridine-functionalized clusters **2** and **5**, respectively. The crystal structure of hybrid **2** was communicated previously.[16] Hybrid **5** was characterized by ^{1}H NMR spectroscopy (see Experimental Section), electrospray ionization mass spectrometry (ESI-MS), and X-ray single-crystal diffraction.

The mass spectrum of **5** shows isotopic clusters centered at *m*/*z* 853.05 (100), 1707.73 (9), and 1953.09 (3%). These signals can be assigned to the cluster anion M^{2-} ($M = [Mo_6O_{17}N_8C_{58}H_{52}]$, calcd *m*/*z*: 854.36), $M^{2-}+H^+$ (calcd *m*/*z*: 1709.72), and $M^{2-}+Bu_4N^+$ (calcd *m*/*z*: 1952.17), respectively, consistent with its structure.

Hybrid **5** crystallizes in the triclinic space group $P\bar{1}$[17] with two formula units per asymmetric unit of the cell. The anions of the two formula units adopt rather different configurations (Figure 1). Most notable are the different dihedral angles between one terpyridine system (2-3-4) and the adjacent phenyl ring (ring 1). In configuration a, the dihedral angle between rings 1 and 2 is only 19.7°, while the corresponding two rings are nearly perpendicular to each other in configuration b.

Coordination of hybrids **2** and **5** with Fe^{2+} was carried out in acetonitrile or dimethyl sulfoxide (DMSO) at room temperature. ^{1}H NMR titration (see Supporting Information (SI) for details) indicates that the terpyridine ligand in **2** almost completely coordinates with Fe^{2+} to form Fe^{2+} bis(terpyridine) complex when 0.5 equiv of Fe^{2+} (vs **2**) is added. Further addition of Fe^{2+} does not result in the dissociation of the bis(terpyridine) complex; this indicates a high kinetic barrier and thus kinetic inertness of $[Fe(tpy)_2]^{2+}$ complexes.[18] Hybrid **3**, however, has a net −2 charge. Excess Fe^{2+} can replace Bu_4N^+ and form ion pairs with **3**. Indeed, when an excess of $FeCl_2$ (10 equiv) was added to a solution of **2** in acetonitrile, a green precipitate immediately formed,

[*] J. Kang, Dr. B. Xu, Prof. Z. Peng, Dr. X. Zhu
Department of Chemistry
University of Missouri-Kansas City
Kansas City, MO 64110 (USA)
Fax: (+1) 816-235-5502
E-mail: pengz@umkc.edu
Dr. Y. Wei
Department of Chemistry
Tsinghua University
Beijing, 100080 (China)
Dr. D. R. Powell
Department of Chemistry
University of Kansas
Lawrence, KS 66045 (USA)

[**] This work is supported by National Science Foundation (DMR 0134032) and the Office of Naval Research. We thank Dr. Nathan D. Leigh for the ESI-MS measurements on hybrid **5**.

Supporting information for this article is available on the WWW under http://www.angewandte.org or from the author.

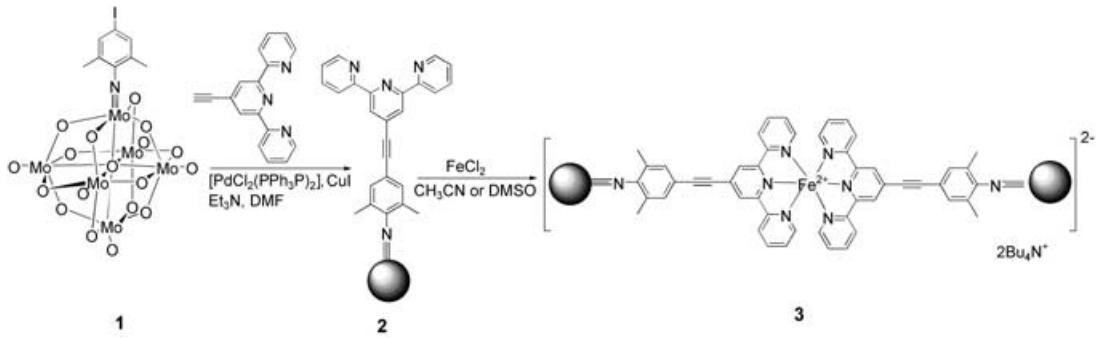

Scheme 1. Synthesis of a molecular hybrid containing POM clusters and a transition-metal complex linked by a conducting bridge.

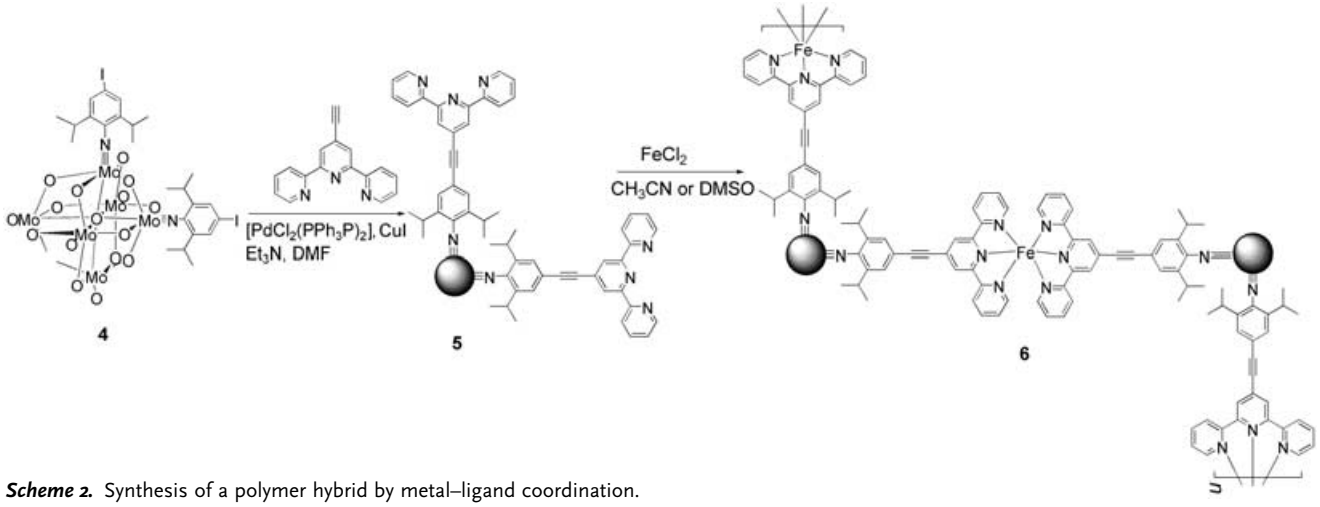

Scheme 2. Synthesis of a polymer hybrid by metal–ligand coordination.

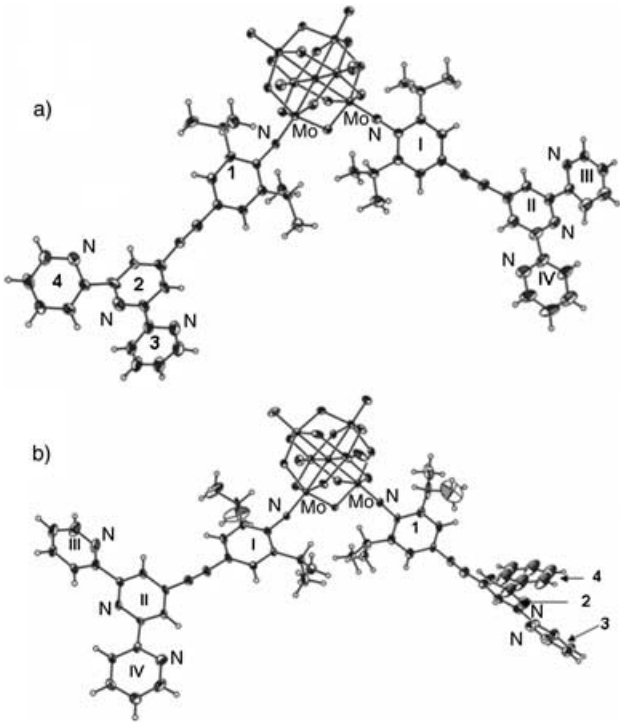

Figure 1. ORTEP representation for the two anion configurations in hybrid **5**. Selected dihedral angles [°]: I–II, 25.1 (a), 25.6 (b); II–III, 18.8 (a), 17.2 (b); II–IV, 6.7 (a), 16.8 (b); 1–2, 19.7 (a), 81.6 (b); 2–3, 3.8 (a), 6.4 (b); 2–4, 35.2 (a), 33.6 (b).

whose ^{1}H NMR spectrum shows no proton signals of Bu_4N^+ (see the Supporting Information). A UV/Vis titration experiment (see the Supporting Information) also points to the formation of **3**-Fe^{2+} ion pairs when an excess of Fe^{2+} is added. These results indicate that, to form **3** with Bu_4N^+ as the counterion, the appropriate ratio of Fe^{2+}/**2** is 1:2.

Hybrid **3** with the Bu_4N^+ counterion is soluble in dimethyl formamide (DMF) and DMSO. Its structure was confirmed by ^{1}H NMR and ESI-MS measurements. As shown in Figure 2, both hybrids **2** and **3** show nearly identical signals in the region of chemical shifts between 0 and 4 ppm, where protons in the Bu_4N^+ counterion (labeled a, b, c, d) and the benzyl methyl protons (proton 8) appear. The cluster-bound aryl protons (proton 7) also exhibit similar chemical shifts. Protons in the terpyridine ligands, however, show drastic changes in chemical shifts after Fe^{2+}–terpyridine coordination. By comparison with the ^{1}H NMR spectrum of Fe^{2+}–bis(terpyridine) model complex **7**, one can clearly identify the similarity in the aromatic region between **3** and **7**, assign all signals accordingly, and thus unambiguously confirm Fe^{2+}–terpyridine complexation. The lack of signals corresponding to free terpyridine ligands in the ^{1}H NMR spectrum of **3** indicates rather complete coordination. The integration ratio of signals associated with the hybrid anion versus those corresponding to the counterion also offers useful structural information. For example, the integration ratios of signal 3′ over b are 1:7.76 for **2** and 1:3.82 for **3**, that is, one Fe^{2+} ion

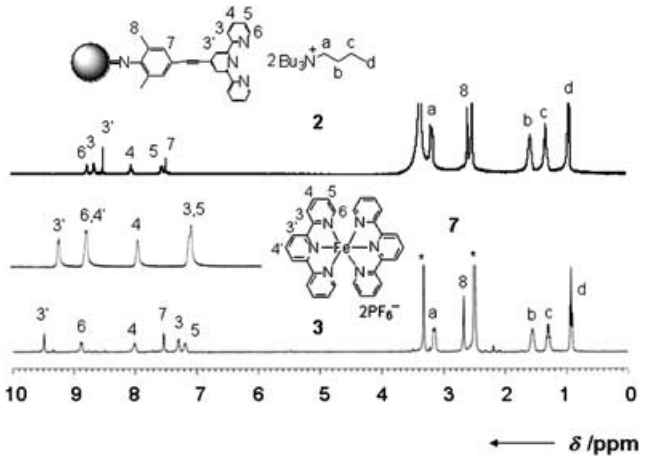

Figure 2. ^{1}H NMR spectra of **2** and **3**. The middle spectrum is the ^{1}H NMR spectrum of **7**. All spectra were recorded in [D$_6$]DMSO.

indeed binds to two terpyridyl ligands (the theoretical ratios of 3′ over b for **2** and **3** are 1:8 and 1:4, respectively).

The structure of **3** is also confirmed by ESI-MS measurements. The ESI mass spectrum of hybrid **3** shows two major isotopic clusters centered at *m*/*z* 1265 and 1239.2. The first signal can be assigned to the cluster anion M^{2-} of **3** (M^{2-} = $[Mo_{12}O_{36}N_8C_{50}H_{36}Fe]^{2-}$, calcd *m*/*z*: 1266.0), while the second is attributed to hybrid **2** ($[\mathbf{2}]^{2-} + H^+$, $[Mo_6O_{18}N_4C_{25}H_{19}]^-$, calcd *m*/*z*: 1239.1). The relative intensity of these two signals depends strongly on probe potential. Under relatively high probe potential (15 V), the signal corresponding to free hybrid ligand **2** dominates (1239.2, 100%; 1265, 55%), while under low probe potential (8 V), the relative intensity of the two signals reverses (1239.2, 38 % %; 1265, 100%); hence, the appearance of signals corresponding to noncoordinated hybrid **2** is due to in-source decomposition of **3**. Great efforts were made to grow single crystals of **3**, but all attempts so far were unsuccessful.

Unlike **3**, coordinated hybrid **6** exhibits poor solubility in common organic solvents. When the coordination of **5** with $FeCl_2$ is carried out in acetonitrile, the coordinated product precipitates immediately as a green solid, and the overlying clear solution becomes colorless. ^{1}H NMR measurements on the clear solution show no signals for aromatic proton but only for tetrabutylammonium counterion, indicating that all starting hybrid **5** has reacted and precipitated. Hybrid **6** does show slight solubility in DMSO, however. When the coordination process of hybrid **5** with $FeCl_2$ was carried out in [D$_6$]DMSO, a green precipitate was again produced. The color of the solution, however, remained green. After mixing with $FeCl_2$ for only 20 min, the ^{1}H NMR spectrum of the solution (see the Supporting Information) shows that the signals corresponding to free terpyridine ligands have completely disappeared, that is, all terpyridine ligands have coordinated with Fe^{2+}. The peaks in the aromatic region show chemical shifts nearly identical to those of hybrid **3**, further confirming the formation of iron(II)–bis(terpyridine) complexes. The overwhelming counterion signals in the solution indicate that, as coordinated hybrid **6** precipitates from solution, the tetrabutylammonium counterion remains.

Indeed, the ^{1}H NMR spectrum of **6** (the green precipitate), obtained after days of data collection due to its poor solubility, shows no signals attributable to the counterion, while signals consistent with iron(II)–bis(terpyridine) complex can be identified. Note that the lack of free terpyridyl ligands in **6** may also indicate the formation of cyclic oligomers.

The electronic properties of hybrids **3** and **6** were studied by UV/Vis absorption measurements. As shown in Figure 3,

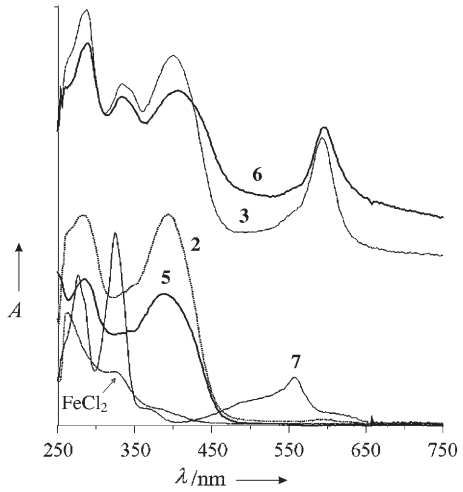

Figure 3. UV/Vis absorption spectra of hybrids **2**, **3**, **5**, **6**, and model Fe^{2+}–bis(terpyridine) complex **7** in DMSO.

terpyridine-anchored clusters **2** and **5** both show a maximum absorption at 392 nm, which is assigned to the ligand-to-metal charge-transfer (LMCT) transition associated with Mo–N π bonding. After coordination with Fe^{2+}, the resulting hybrids **3** and **6** show two new absorption bands, one at 595 nm and the other at 333 nm. The first band is attributed to MLCT, while the second is due to the ligand-centered (LC) transition, both associated with the Fe^{2+}–bis(terpyridine) complex. These assignments are confirmed by the UV/Vis absorption spectrum of model complex **7**, which shows two similar absorption bands. The MLCT bands of **3** and **6** are red-shifted by nearly 40 nm compared to that of **7**. The electron-withdrawing nature of the Mo≡N bond lowers the π* orbital of the ligand and thus decreases the MLCT band gap and results in its bathochromic shift.[19] The more extended π conjugation of the ligands in **3** and **6** than in **7** also contributes to the red shift.[20]

The electrochemical behavior of hybrids **3** and **6** was studied by cyclic voltammetry. Figure 4 shows the cyclovoltammogram of **6**, measured on its polymer film, together with those of **3**, model complex **7**, and hybrid **2**, measured in DMSO solutions. In the range −2.0–1.5 V (vs Ag/Ag^+), **7** shows one metal-localized (Fe^{2+}/Fe^{3+}) reversible oxidation wave at 0.805 V ($\Delta E = 0.11$ V) and two ligand-localized reversible reduction waves at −1.47 V ($\Delta E = 0.10$ V) and −1.62 V ($\Delta E = 0.10$ V).[21] In the same potential range, hybrid **2** exhibits no oxidation process. Besides one semireversible reduction process at −1.60 V, which can be attributed to the reduction of the terpyridine ligand, a reversible reduction wave at a much lower potential of −0.80 V ($\Delta E = 0.17$ V) is

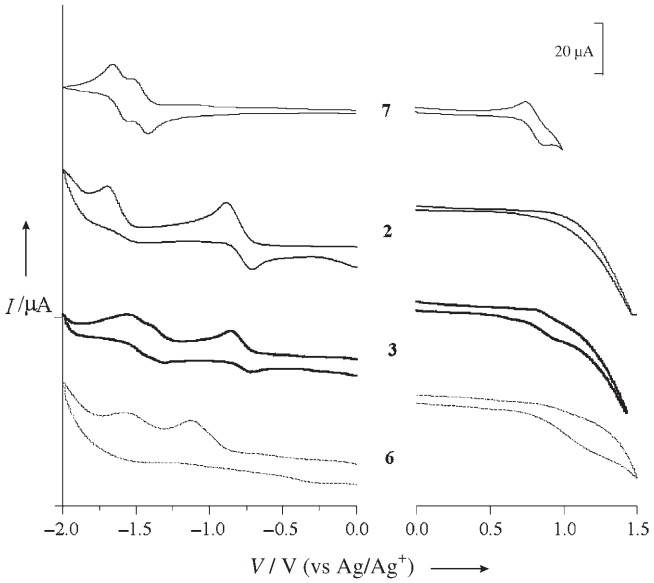

Figure 4. Cyclic voltammograms of **2**, **3**, and **7**.

observed. This reduction process is associated with the POM cluster.[7] Under the same conditions and in the same potential range, hybrid **3** shows redox waves of both **2** and **7**. The observation of the $Fe^{2+/3+}$ oxidation wave, the POM-associated reduction wave, and the two ligand-centered reduction waves once again confirms the structure of **3**. For **6**, the $Fe^{2+/3+}$ oxidation wave is still noticeable, and the reduction peak at −1.12 V is consistent with diimido derivatives of POMs.[7,12]

In conclusion, we have successfully prepared the first hybrid in which a POM cluster and transition-metal complexes are linked through an extended π-conjugated bridge. A coordinated POM-containing hybrid polymer is also demonstrated. The hybrids exhibit low-lying MLCT transitions associated with the transition-metal complexes and LMCT transitions located at the cluster/organic Mo≡N junction. This rational building-block approach may be extended to the preparation of hybrids with other metal ions, particularly those coordinating with terpyridine ligands at room temperature with large binding constants.

Experimental Section

See the Supporting Information for detailed synthetic procedures of hybrids **3**, **5**, and **6**, their ^{1}H NMR spectra, ^{1}H NMR titration and UV/Vis titration of the coordination process of **2** with $FeCl_2$, and ESI-MS data of **5** and **3**.

Received: June 2, 2005
Published online: October 5, 2005

Keywords: C–C coupling · iron · molybdenum · organic–inorganic hybrids · polyoxometalates

[1] a) P. Gouzerh, A. Proust, *Chem. Rev.* **1998**, *98*, 77, and references therein; b) P. Gouzerh, R. Villanneau, R. Delmont, A. Proust, *Chem. Eur. J.* **2000**, *6*, 1184.

[2] a) D. Hagraman, C. Zubieta, D. J. Rose, J. Zubieta, R. C. Haushalter, *Angew. Chem.* **1998**, *109*, 904; *Angew. Chem. Int. Ed.* **1998**, *36*, 873; b) V. Shivaiah, M. Nagaraju, S. K. Das, *Inorg. Chem.* **2003**, *42*, 6604; c) X. B. Cui, J. Q. Xu, H. Meng, S. T. Zheng, G. Y. Yang, *Inorg. Chem.* **2004**, *43*, 8005.

[3] a) R. S. Rarig, Jr., L. Bewley, V. Golub, C. J. O'Conner, J. Zubieta, *Inorg. Chem. Commun.* **2003**, *6*, 539; b) A. Dolbecq, P. Mialane, L. Lisnard, J. Marrot, F. Sécheresse, *Chem. Eur. J.* **2003**, *9*, 2914; c) C. D. Wu, C. Z. Lu, H. H. Zhuang, J. S. Huang, *J. Am. Chem. Soc.* **2002**, *124*, 3836.

[4] a) S. I. Stupp, P. V. Braun, *Science* **1997**, *277*, 1242; b) O. M. Yaghi, H. Li, C. Davis, D. Richardson, T. L. Groy, *Acc. Chem. Res.* **1998**, *31*, 474.

[5] a) Y. Lin, R. G. Finke, *J. Am. Chem. Soc.* **1994**, *116*, 8335; b) K. Takahashi, M. Yamaguchi, T. Shido, T. Ohtani, K. Isobe, M. Ishigawa, *J. Chem. Soc. Chem. Commun.* **1995**, 1301; c) R. Neumann, M. Dahan, *Nature* **1997**, *388*, 353.

[6] I. Bar-Nahum, H. Cohen, R. Neumann, *Inorg. Chem.* **2003**, *42*, 3677.

[7] J. B. Strong, G. P. A. Yap, R. Ostrander, L. M. Liable-Sands, A. L. Rheingold, R. Thouvenot, P. Gouzerh, E. A. Maatta, *J. Am. Chem. Soc.* **2000**, *122*, 639.

[8] a) A. R. Moore, H. Kwen, A. B. Beatty, E. A. Maatta, *Chem. Commun.* **2000**, 1793; b) B. Xu, Y. Wei, C. L. Barnes, Z. Peng, *Angew. Chem.* **2001**, *113*, 2353; *Angew. Chem. Int. Ed.* **2001**, *40*, 2290.

[9] J. L. Stark, V. G. Young, Jr., E. A. Maatta, *Angew. Chem.* **1995**, *107*, 2751; *Angew. Chem. Int. Ed. Engl.* **1995**, *34*, 2547.

[10] M. Lu, Y. Wei, B. Xu, C. F.-C. Cheung, Z. Peng, D. Powell, *Angew. Chem.* **2002**, *114*, 1636; *Angew. Chem. Int. Ed.* **2002**, *41*, 1566.

[11] J. Kang, J. Nelson, M. Lu, B. Xie, Z. Peng, D. R. Powell, *Inorg. Chem.* **2004**, *43*, 6408.

[12] M. Lu, B. Xie, J. Kang, F. Chen, Y. Yang, Z. Peng, *Chem. Mater.* **2005**, *17*, 402.

[13] a) A. Juris, V. Balzani, F. Barigelletti, S. Campagna, P. Belser, A. von Zelewsky, *Coord. Chem. Rev.* **1988**, *84*, 85; b) S. Baitalik, X. Wang, R. H. Schmehl, *J. Am. Chem. Soc.* **2004**, *126*, 16304.

[14] Y. Wei, B. Xu, C. L. Barnes, Z. Peng, *J. Am. Chem. Soc.* **2001**, *123*, 4083.

[15] L. Xu, M. Lu, B. Xu, Y. Wei, Z. Peng, D. R. Powell, *Angew. Chem.* **2002**, *114*, 4303; *Angew. Chem. Int. Ed.* **2002**, *41*, 4129.

[16] a) B. Xu, Z. Peng, Y. Wei, D. R. Powell, *Chem. Commun.* **2003**, 2562; b) Z. Peng, *Angew. Chem.* **2004**, *116*, 948; *Angew. Chem. Int. Ed.* **2004**, *43*, 930.

[17] Crystal data for **5**: $2(C_{16}H_{36}N)^+(C_{58}H_{52}Mo_6N_8O_{17})^{2-}(CH_2Cl_2)$, $M_r = 2278.56$, triclinic, $P\bar{1}$, $a = 16.296(3)$, $b = 19.855(4)$, $c = 30.823(6)$ Å, $\alpha = 90.452(4)$, $\beta = 93.885(4)$, $\gamma = 90.316(4)°$, $V = 9950(3)$ Å^3, $Z = 4$, $Z' = 2$, $\rho_{calcd} = 1.521$ g cm^{-3}, $T = 100(2)$ K, $R1 = 0.0711$, and $wR2 = 0.1973$. GOF $(F^2) = 1.049$. CCDC-272303 contains the supplementary crystallographic data for this paper. These data can be obtained free of charge from the Cambridge Crystallographic Data Centre via www.ccdc.cam.ac.uk/data_request/cif.

[18] a) S. Schmatloch, A. M. J. van den Berg, A. S. Alexeev, H. Hofmeier, U. S. Schubert, *Macromolecules* **2003**, *36*, 9943; b) R. Dobrawa, M. Lysetska, P. Ballester, M. Grüne, F. Würthner, *Macromolecules* **2005**, *38*, 1315.

[19] E. C. Constable, A. M. W. Cargill Thompson, *J. Chem. Soc. Dalton Trans.* **1994**, 1409.

[20] S. Bernhard, J. I. Goldsmith, K. Takada, H. D. Aruña, *Inorg. Chem.* **2003**, *42*, 4389.

[21] S. Bernhardt, K. Takada, D. J. Díaz, H. D. Aruña, H. Mürner, *J. Am. Chem. Soc.* **2001**, *123*, 10265.

